Projection of the Impact of Climate Change on the Surface Energy and Water Balance in the Seyhan River Basin Turkey

Kenji TANAKA[1], Yoichi FUJIHARA[2] and Toshiharu KOJIRI[3]

[1]*WRRC, DPRI, Kyoto University, Gokasho, Uji, 611-0011, Japan*
[2]*RIHN, 457-4 Motoyama, Kamigamo, Kita-ku, Kyoto 603-8047, Japan*
[3]*WRRC, DPRI, Kyoto University, Gokasho, Uji, 611-0011, Japan*

1.　Introduction

In this study, estimation of the surface energy and water balance components and related hydrological variables of the Seyhan River basin Turkey is attempted through the off-line simulation of the LSM (Land Surface Model) forced by the product of the RCM (Regional Climate Model) for both present and future (warm-up) condition. To assess the impact of climate change on agricultural production system including human reaction (farm management, cropping patterns, etc.), three patterns of landuse scenario are used in the numerical simulation. Furthermore, two kind of future climate scenarios are applied to reduce the uncertainty in the assessment of surface energy and water balance.

2.　Basin Characteristics

Detailed physical boundary of the Seyhan basin was carefully defined by Turkish group according to the large scale maps. Landuse/landcover dataset was produced from satellite images of Landsat (see the report of Vegetation sub-group). According to this dataset, current four major landcover conditions of the Seyhan basin are grassland (31.74%), dry cropland (22.22%), evergreen needleleaf forest (19.37%), and irrigated cropland (15.21%).

Several soil physical parameters such as porosity, field capacity, root zone depth, etc. are also extracted from ECOCLIMAP (http://www.cnrm.meteo.fr/gmme/). ECOCLIMAP is a new global dataset at a 1 km resolution. It is intended to be used to initialize model parameters in LSMs.

3.　SiBUC and irrigation scheme

SiBUC (Simple Biosphere including Urban Canopy)[3] land surface scheme was designed to treat the landuse condition (natural vegetation, cropland, urban area, water body) in detail. Especially irrigation scheme for the various kinds of cropland is implemented[4]. Basic concept of the irrigation scheme is to maintain the soil moisture within appropriate ranges which are defined for each growing stage of each crop type. The irrigation rules for cropland are described by seeding (planting) date, harvesting date, the periods of each growing stage, lower limit of soil wetness in each growing stage, and amount of water supplied in one time. As a default parameter, lowest values of soil wetness for each growing stage and each crop type are prepared from agricultural manual in China.

In this study, maize and citrus are selected as representative of various irrigated crops. According to the information from Irrigation and Drainage sub-group, irrigation period for maize and citrus are from May 23 to Aug 6, from May 14 to Oct 9, respectively. For the future climate simulation, growing period is shorten by 10 days considering the faster growth in warmer condition. **Table 1** shows a date (DOY: day of year) of growing period used for present and future simulations.

Table 1 : Start and end of irrigation period

		start	end	period
present	maize	143	218	75
	citrus	134	282	148
future	maize	143	208	65
	citrus	134	272	138

4.　Experimental design

The product of RCM (8.3km product) is utilized as forcing of land suface model. Seven meteorological components (precipitation, downward short-wave and long-wave radiation, wind speed, air temperature, specific humidity, pressure) are
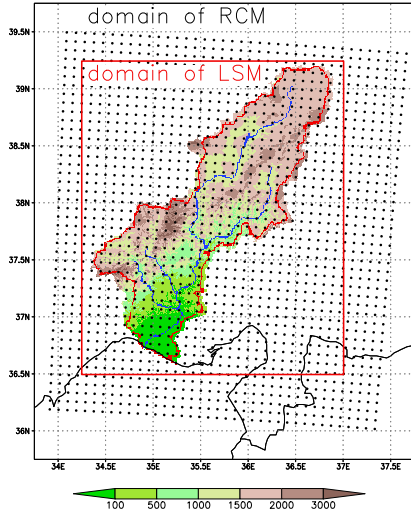
Fig. 1 : Model domain of RCM and LSM

Table 2 : Climate and landuse condition for each simulation

runname	climate	landuse
P0	present	current
M0	warmup (MRI)	no adaptation
M1	warmup (MRI)	adaptation 1
M2	warmup (MRI)	adaptation 2
C0	warmup (CCSR)	no adaptation
C1	warmup (CCSR)	adaptation 1
C2	warmup (CCSR)	adaptation 2

Table 3 : Fraction of four major landcover class for each landuse scenario

	Forest	Grass	Irrigated	Drycrop
A0	19.37	31.74	15.21	22.22
A1	19.37	53.97	13.45	0.00
A2	16.44	34.67	16.51	20.92

Forest: Evergreen Nedleleaf Forest
Grass: grassland, short vegetation
Irrigated: Irrigated farmland (total)
Drycrop: rain-fed wheat

available in hourly time interval.

The simulation period is from 1994 to 2003 for present climate condition. The amount of precipitation during this period is normal. Also, future climate condition (2070's) is produced by so called 'pseud warm-up' method. In this method, boundary condition for RCM is assumed by a linear coupling of the re-analysis data (observation) and the trend component of the global warming estimated by GCM. In this way, pseud warm-up utilizes the synoptic scale variability of the current condition (observation). Since the period is only ten years, the projected future climate condition does not necessarily mean the 'average' future condition. Considering that the original present condition is situated in 'normal' condition, provided future condition is also regarded to be normal.

For future climate condition, two products were produced from different GCM results (MRI and CCSR). For the landcover condition, three land use scenarios (A0:no adaptation, A1:adaptation 1, A2: adaptation 2) are provided. By the combination of climate condition and landuse scenario, 6 simulations were conducted for future. **Table 2** is a summary of the simulation condition and the name of each simulation.

Fig. 1 shows the model domain of RCM and land surface model (LSM). Model domain of RCM covers the whole Seyhan River basin, and 2.75 degree × 2.75 degree area (E34.25-37.0, N36.5-N39.25) is selected as simulation domain for LSM. This area is divided by each 5 min (about 10km) grid boxes (33 × 33 grids). SiBUC uses mosaic approach to incorporate all kind of land-use. **Fig. 3** shows the fraction of four major landcover conditions for each landuse scenario, and basin average landcover fraction is summarized in **Table 3**.

5. Vegetation dynamics

Satellite derived vegetation indices such as NDVI (Normarized Difference Vegetation Index), especially its time series, is very useful and powerful for describing the actual land-surface status[1]. Here, NDVI is a common index to express the activity of vegetation.

SPOT VEGETATION Product (http://free. vgt.vito.be/) is utilized to well express vegetation dynamics. This is a 10-day composite dataset which has about 1km resolution. The included cloud noises were removed by BISE[2] method. Furthermore, average seasonal cycle dataset was produced from the collected 6-years period (from 1999 to 2004). Leaf area index (LAI) is calculated from NDVI and vegetation class. Other time-varying vegetation parameters such as greeness fraction (Nc), vegetation coverage (Vc) are extracted from ECOCLIMAP database. Since SiBUC adopts mosaic scheme to take subgrid

scale heterogeneity into account, these vegetation parameters are aggriated within each landcover class in each LSM grid (10km). Owing to these datasets, spatial distribution and time evolution of vegetation parameters can be well described.
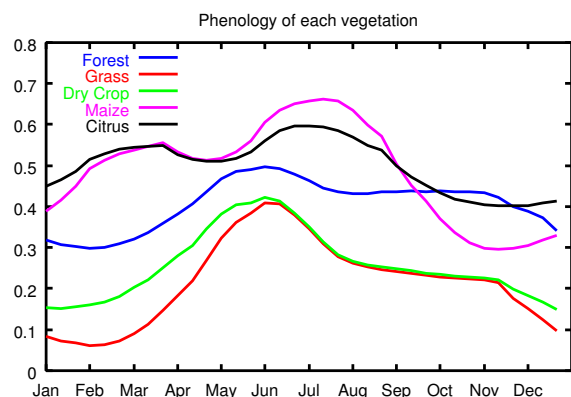

Fig. 2 : Average seasonal cycle of NDVI for each vegetation type

On the other hand, there is no reliable information about the vegetation status in future climate condition. As for future landuse, three scenarios are prepared (A0, A1, A2). To be consistent with landcover condition, vegetation parameters must be changed accordingly when that pixel is change from current landcover. According to current landcover information, average seasonal cycles of vegetation parameters (NDVI, Nc, Vc) are calculated for each vegetation type. Then, they are allocated to landcover changed pixels (1km) in A1 and A2 scenario. **Fig. 2** shows average seasonal cycles of NDVI for each vegetation type. Same parameter values are allocated to remaining pixels (same landcover as current). Finally, these parameters are aggregated for each landcover class in each LSM grid (10km).

6. Results and Discussions

Fig. 5 to **Fig. 8** show the annual (10-year average) water balance components (precipitation, runoff, snowfall, maximum SWE (Snow Water Equivalent), respectively) for present climate and their difference in **M0** and **C0** simulations. **Figs. 9** and **10** show the annual (10-year average) evaporation and irrigation water for present climate, and they compare the difference of climate change impact in **A1** and **A2** landuse scenario.

Annual precipitation of present climate is about 400mm in the upstream region, above 1000mm in the middle region, and about 700mm in the Seyhan delta (**Fig. 5(a)**). As for the impact, precipitation will decrease in the whole Seyhan basin, especially, reduction is more than 250mm in the middle and delta region for both **M0** and **C0** simulations. Runoff also decreases as a result of reduction of precipitation, and the impact is especially large in the high mountain region due to the increase of evaporation (**Figs 9(b)(c)**).

As for snowfall, reduction is larger in **C0** simulation mainly because of warmer temperature. As a result, maximum SWE is projected to decrease more in **C0** simulation. **Fig. 4** shows the seasonal evolution of total amount of water stored as snow in whole Seyhan basin for present and future climate. Maximum SWE is almost 0.4 Gt in present climate, while it will decrease as small as 0.1 Gt in future climate. Here future climate is a mean of **M0** and **C0** simulation.

As for the Seyhan delta (irrigated area), annual evaporation is about 800mm, and about 500mm of irrigation water must be supplied to keep the soil wetness during the growing season in hot and dry summer. Although precipitation will decrease in the whole Seyhan basin, some part of evaporation will increase. Such area coincides with the area where SWE will decrease so much. As a result of reduction of snow cover, those area will receive more short-wave radiation (albedo effect). These energy will contribute to the increase of evaporation in spring season (see **Fig .12**). The difference between **Fig .9(b)** and **Fig .9(c)** is large where irrigated area is abandoned and dry cropland is converted into grassland. Although the growing period is shorten, irrigation water is projected to increase by the higher evaporation demand in the growing season, and the reduction of soil moisture at the begining of growing period (see **Fig .13**).

As a basin average, annual water balance components for present and future climate condition for each landuse scenario are summarized in **Table 4**. Precipitation is projected to decrease about 170mm, while evapotranspiration and runoff decreases about 40mm and 110mm, respectively. Considering the amount of current water balance component, the impact on runoff is significantly large.

Table 4 : Basin average annual water balance components

unit:mm	Present	Future(A0)	Future(A1)	Future(A2)	diff(A0)	diff(A1)	diff(A2)
Prec	634.0	464.3	464.3	464.3	-169.7	-169.7	-169.7
Evap	411.3	373.9	365.4	378.9	-37.5	-45.9	-32.4
Runoff	281.6	168.9	168.1	170.4	-112.6	-113.5	-111.2
Irrig	53.8	69.7	60.4	76.4	15.9	6.6	22.5
delS	-5.0	-8.7	-8.8	-8.7	-3.7	-3.7	-3.6

To see the impacts from climate change for each landcover type, model outputs within the target basin are aggregated according to the dominant landcover condition (dominant landcover is larger than 0.8). **Fig. 11** shows the time series of energy balance components at different landcover (grassland, forest, dry cropland, irrigated crop). In this figure, lines are for present climate and dots are for future climate (average of **M0** and **C0**). In the grassland, net radiation and latent heat becomes larger in May, while sensible heat becomes larger from May to August. In the forest, impact on net radiation is very small. From May to August, latent heat becomes smaller and sensible heat vise versa. In the dry cropland, latent heat becomes larger in winter and spring, while it becomes much smaller in summer. Dry cropland gets much impact on all energy balance components is larger than other landcover. By the way, it must be noticed that most of the dry cropland area are located in the area where the reduction of precipitation is very large. Irrigated crop area is also located in the area where the impact of precipitation is very large. But the impact on surface energy balance is relatively small due to irrigation.

Acknowledgement

REFERENCES

1) Kozan, O., K.Tanaka, S.Ikebuchi and M.Qian : Landuse and cropping pattern classification using satellite derived vegetation indices in the Huaihe river basin, *Proc. of the 2nd International Conference on Hydrology and Water Resources in Asia Pacific Region*, Vol.2, pp.732-740, 2004.

2) Viovy, N. and O.Arino : The best index slope extraction(BISE): A method for reducing noise in NDVI time series, *Int. J. Remote Sens.*, Vol.13, pp.1585-1590, 1992.

3) Tanaka, K. and S. Ikebuchi : Simple Biosphere Model Including Urban Canopy (SiBUC) for Regional or Basin-Scale Land Surface Processes, Proc. of International Symposium on GEWEX Asian Monsoon Experiment, pp.59-62, 1994.

4) Kozan, O., K.Tanaka and S.Ikebuchi : The Estimation of Water and Heat Budget in the Huaihe River Basin China - Detail Representation of Various Cropland and Irrigation -, *Proc. of the 1st International Conference on Hydrology and Water Resources in Asia Pacific Region*, Vol.2, pp.763-768, 2003.
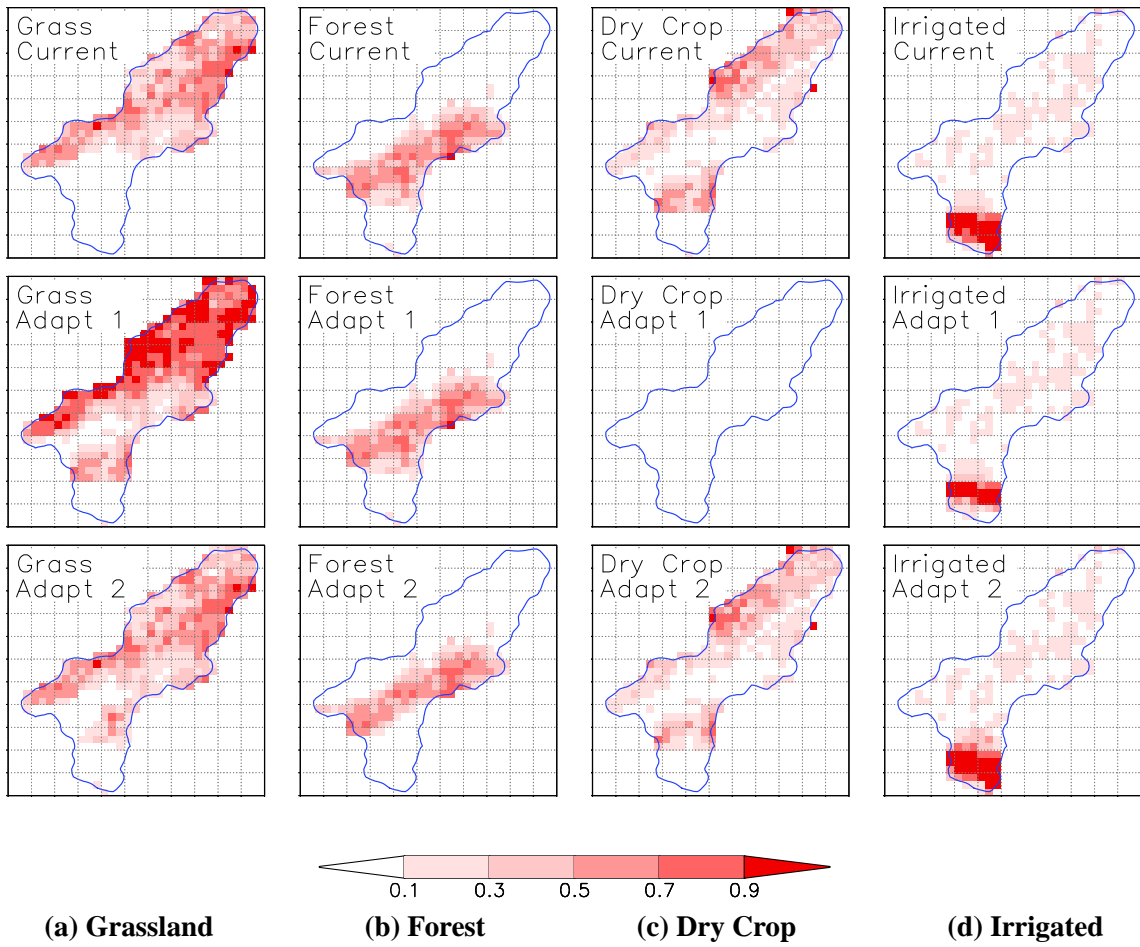
(a) Grassland **(b) Forest** **(c) Dry Crop** **(d) Irrigated**

Fig. 3 : Landcover fraction of each grid (top: Current, middle:Adapt 1, bottom:Adapt 2)
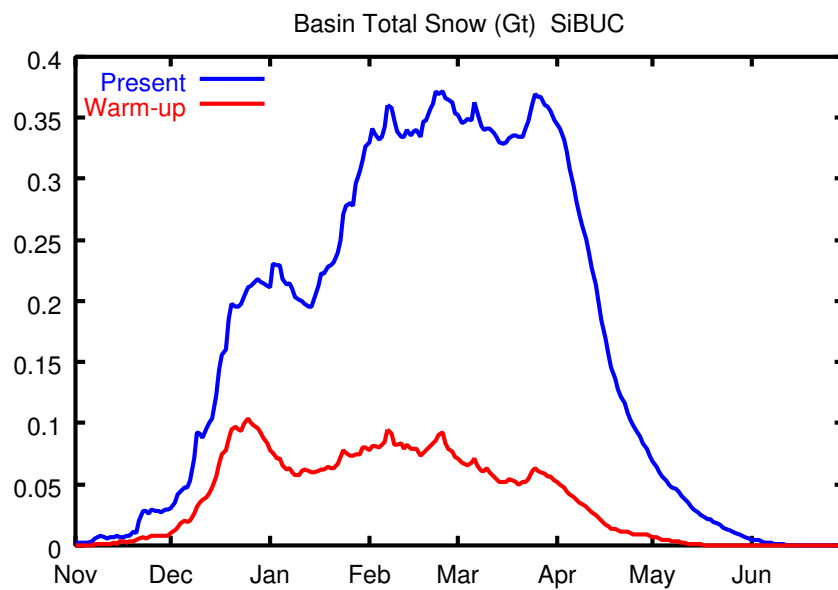
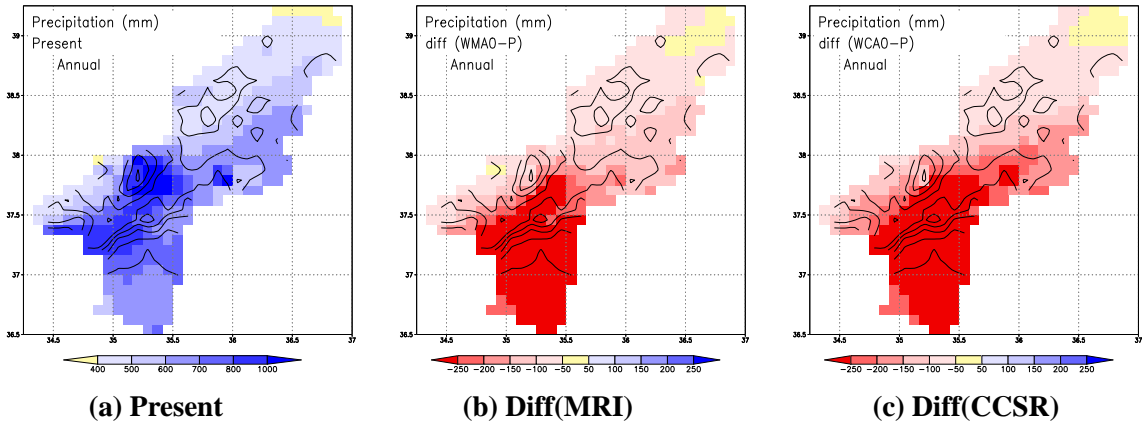**Fig. 4 : Basin total storage of snow (blue:present, red:future)**

(a) Present **(b) Diff(MRI)** **(c) Diff(CCSR)**

Fig. 5 : Annual precipitation of present climate and its difference in MRI and CCSR run

(a) Present **(b) Diff(MRI)** **(c) Diff(CCSR)**
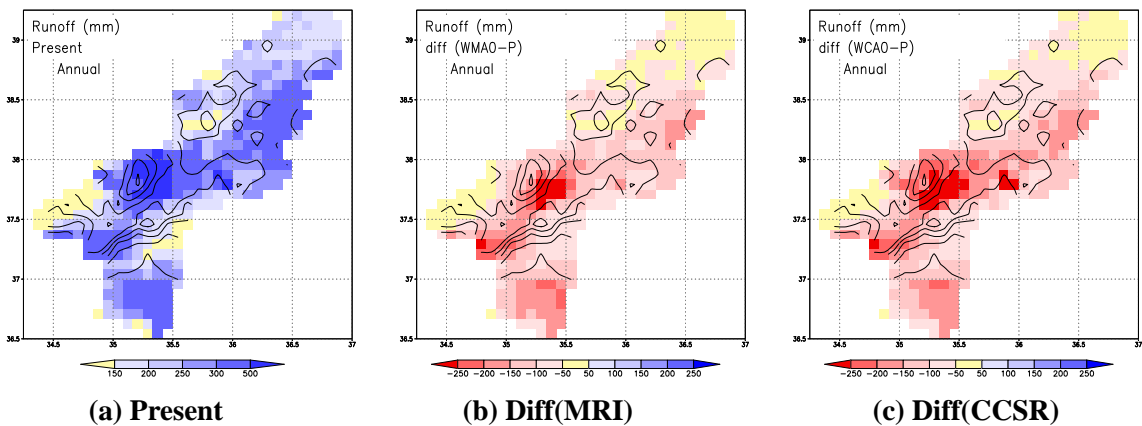
Fig. 6 : Annual runoff of present climate and its difference in MRI and CCSR run

(a) Present **(b) Diff(MRI)** **(c) Diff(CCSR)**
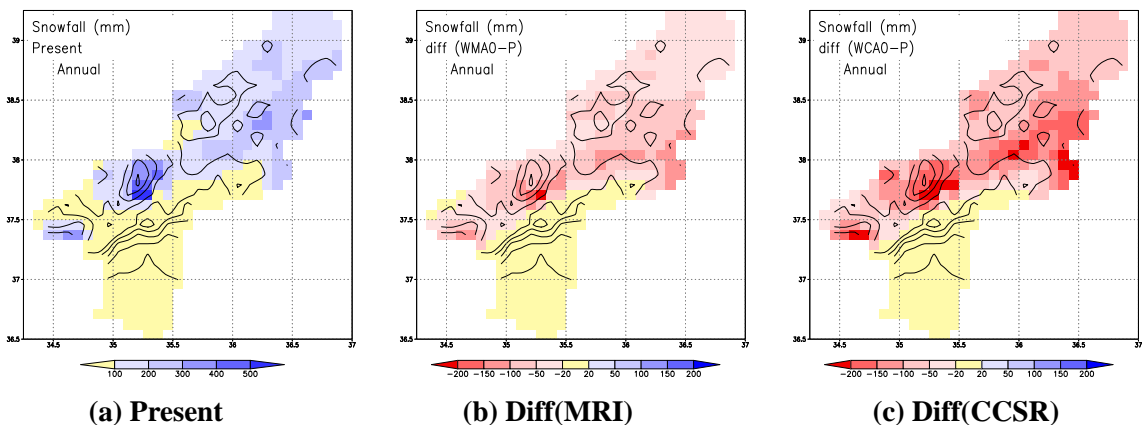
Fig. 7 : Annual snowfall of present climate and its difference in MRI and CCSR run

(a) Present **(b) Diff(MRI)** **(c) Diff(CCSR)**
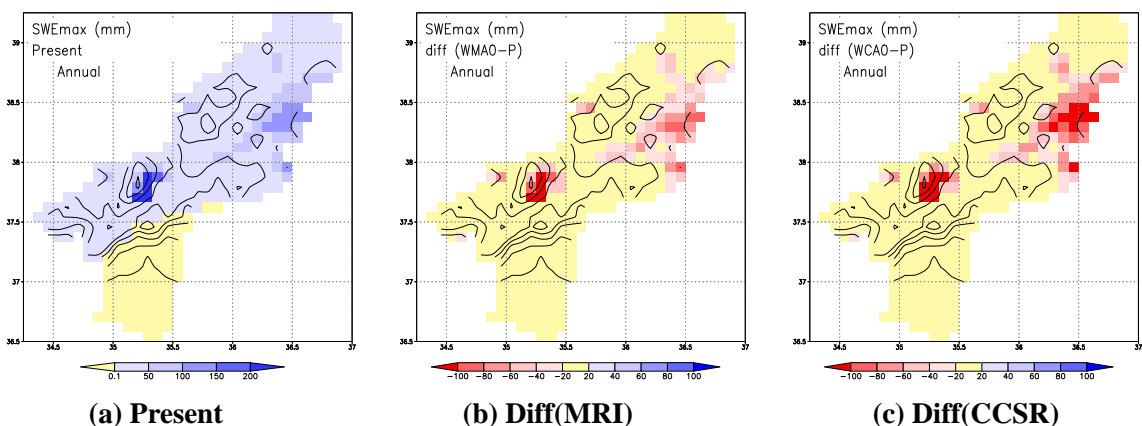
Fig. 8 : Maximum SWE of present climate and its difference in MRI and CCSR run

(a) Present   **(b) Diff(A1)**   **(c) Diff(A2)**
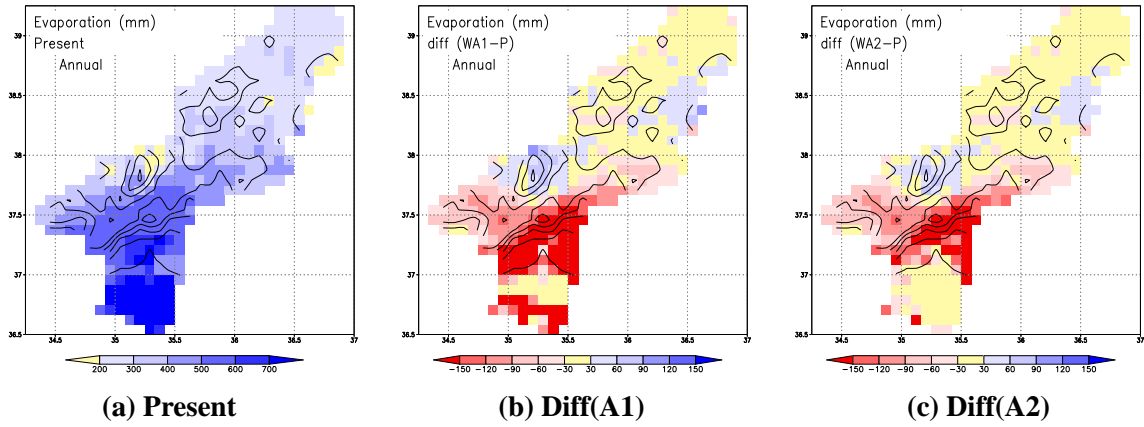
Fig. 9 : Annual evapotranspiration of present climate and its impact in A1 and A2 scenario

(a) Present   **(b) Diff(A1)**   **(c) Diff(A2)**
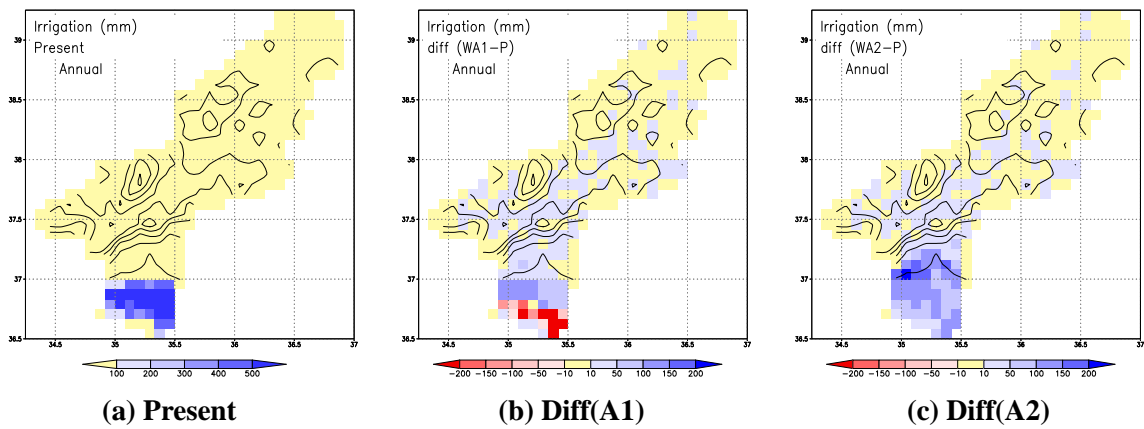
Fig. 10 : Annual Irrigation water of present climate and its impact in A1 and A2 scenario

(a) grassland   **(b) forest**

(c) dry cropland   **(d) irrigated crop**
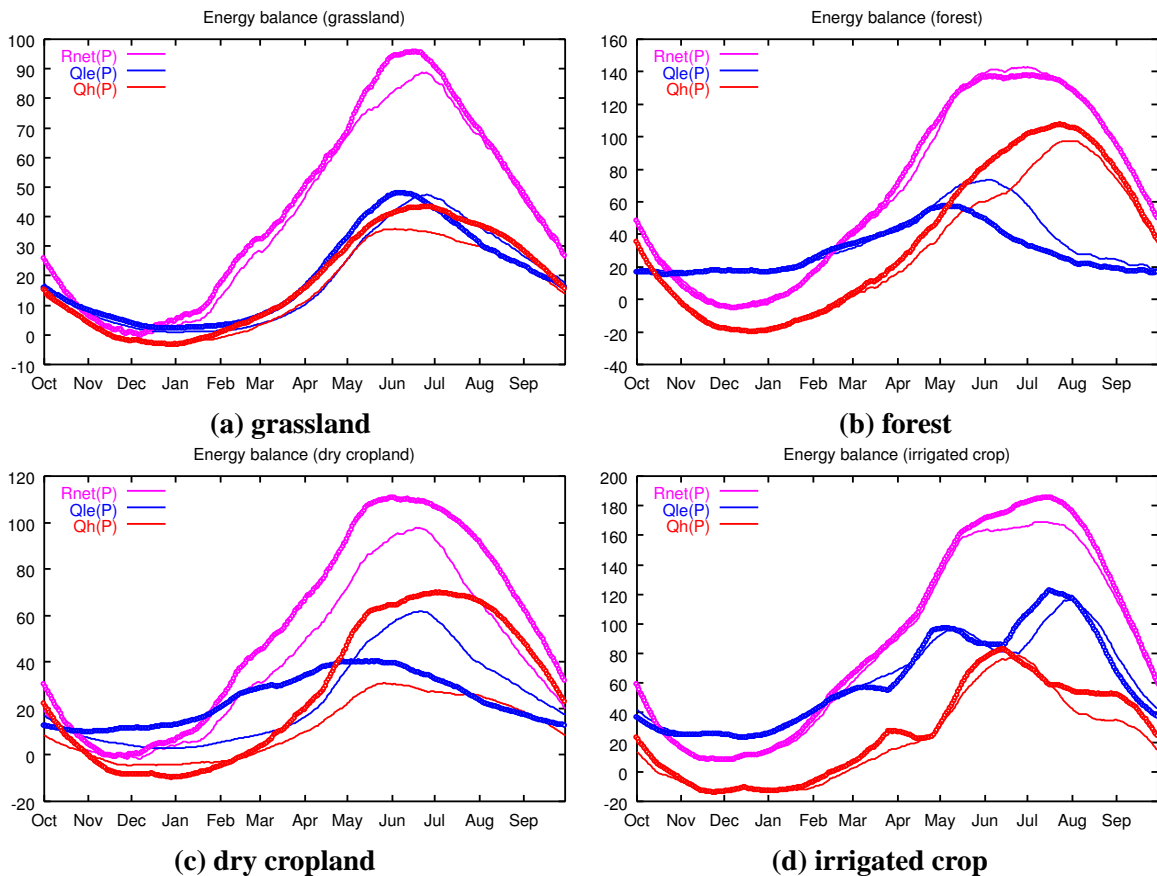
Fig. 11 : Comparison of seasonal cycle of surface energy balance for present and future climate at four different landcover condition (Qle: latent heat, Qh: sensible heat)
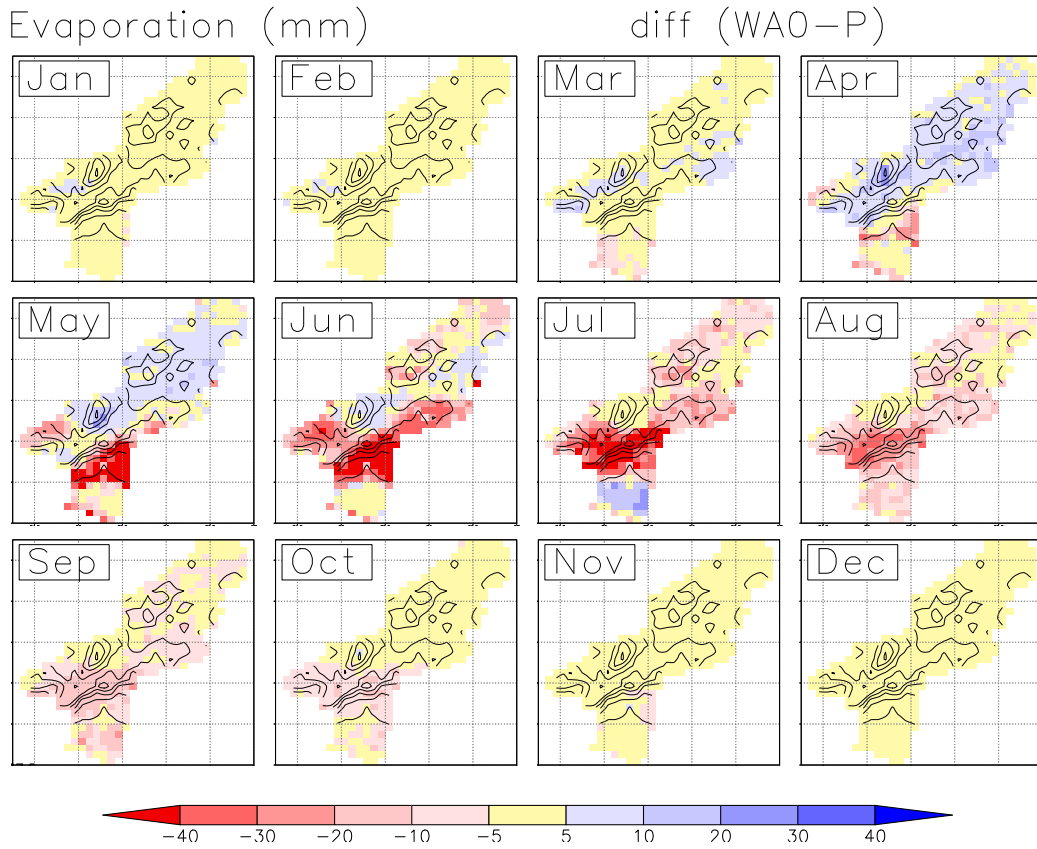**lines: present, dots: future (average of M0 and C0 run)**

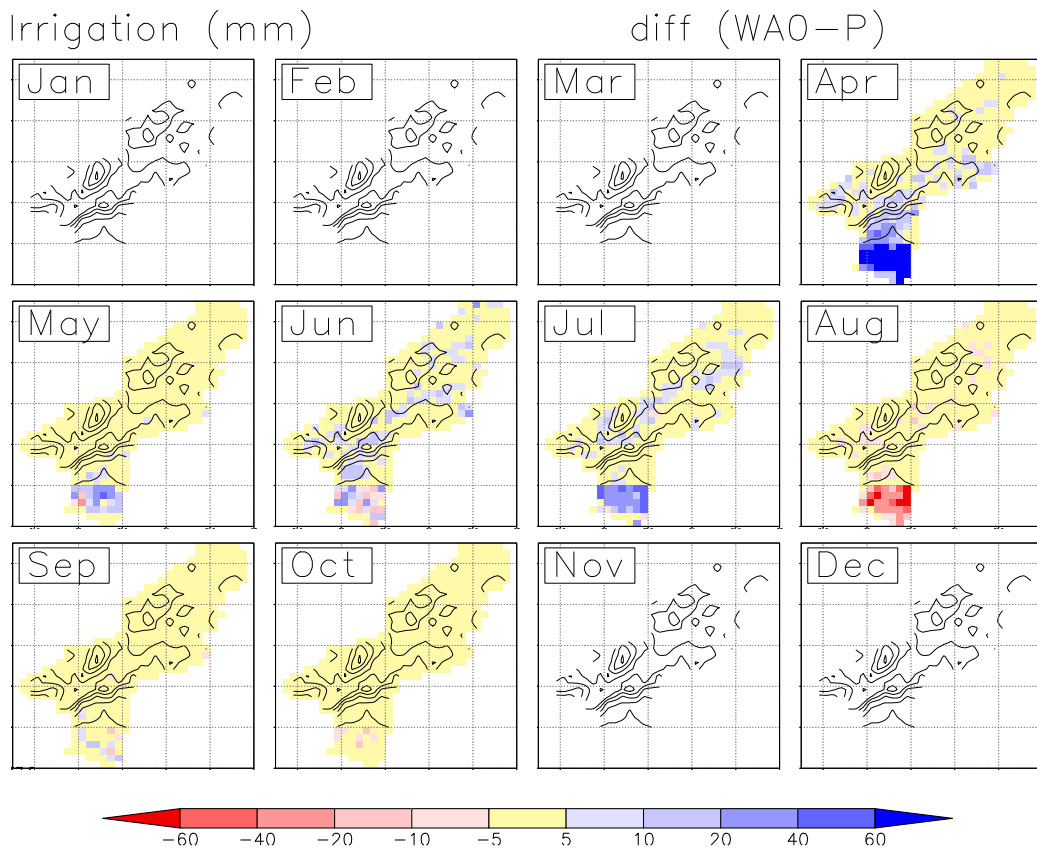**Fig. 12 : Impact of climate change on evaporation at each month**

Fig. 13 : Impact of climate change on irrigation water at each month